

Controlled Synthesis of Poly(neopentyl *p*-styrene sulfonate) via Reversible Addition-Fragmentation Chain Transfer Polymerisation

Isabel Fraga Domínguez,^{a,b,c} Joanna Kolomanska,^c Priscilla Johnston,^c Agnès Rivaton^{a,b} and Paul D. Topham^{c*}

a. Université Blaise Pascal, Institut de Chimie de Clermont-Ferrand, Équipe Photochimie, BP 10448, F-63000 Clermont-Ferrand, France.

b. CNRS, UMR 6296, ICCF, Équipe Photochimie, BP 80026, F-63171 Aubière, France.

c. Chemical Engineering and Applied Chemistry, Aston University, Birmingham, B4 7ET, UK.

* Corresponding author: p.d.topham@aston.ac.uk

Keywords

RAFT polymerisation, poly(*p*-styrene sulfonate), poly(neopentyl *p*-styrene sulfonate), trithiocarbonate, controlled polymerisation, azide-functionalised polymer.

Abstract

The controlled synthesis of poly(neopentyl *p*-styrene sulfonate) (PNSS) using reversible addition-fragmentation chain transfer (RAFT) polymerisation has been studied under a wide range of experimental conditions. PNSS, can be used as an organic-soluble, thermally-labile precursor for industrially valuable poly(*p*-styrene sulfonate), PSS; widely employed in technologies such as ionic exchange membranes and organic electronics. The suitability of

two different chain transfer agents, three solvents, three different monomer concentrations and two different temperatures for the polymerisation of neopentyl *p*-styrene sulfonate is discussed in terms of the kinetics of the process and characteristics of the final polymer. Production of PNSS with systematically variable molecular weights and low dispersities ($\mathcal{D} \leq 1.50$ in all cases) has been achieved using 2-azidoethyl 2-(dodecylthiocarbonothioylthio)-2-methylpropionate in anisole at 75 °C, with initial monomer concentration of 4.0 M. Finally, a poly(neopentyl *p*-styrene sulfonate)-*b*-polybutadiene-*b*-poly(neopentyl *p*-styrene sulfonate) (PNSS-*b*-PBD-*b*-PNSS) triblock copolymer has been synthesised via azide-alkyne click chemistry. Moreover, subsequent thermolysis of the PNSS moieties generated poly(*p*-styrene sulfonate) end blocks. This strategy allows the fabrication of amphiphilic copolymer films from single, organic solvents, without the need for post-deposition chemical treatment.

Introduction

Poly(*p*-styrene sulfonate) (PSS) is an important material in a number of technologies, with application both in its homopolymeric form and incorporated into different copolymers. For instance, it is employed in proton exchange membranes for fuel cells,(1-3) ion exchange materials,(4, 5) in photonic sensors,(6) humidity sensors,(7, 8) oil additives,(9) water softening,(10) polymeric stabilisers for emulsion polymerisation,(11) and various biomedical applications.(12-15) Most notably, perhaps, is its use as a polymeric dopant for conducting polymers such as polypyrrole,(16-18) polyaniline,(19) and, significantly, poly(3,4-ethylenedioxythiophene) (PEDOT).(17, 18, 20) In the latter, the resulting ionomeric mixture,

PEDOT:PSS, is commonly employed in organic electronics, such as organic electrochemical transistors (OECTs),(21) organic photovoltaics (OPVs),(22) or organic light emitting diodes (OLEDs).(23) In these devices, the stable complex created between the negatively charged PSS and the positive PEDOT can be used as either hole transport layers for improvement of charge extraction(20, 22-24) or as organic electrodes, replacing the commonly used inorganic indium tin oxide (ITO).(25) However, the high polarity of PSS and corresponding restriction to polar solvents causes problems in the processing of organic electronics because of conflicts with other apolar device components, such as polythiophenes or fullerene derivatives.(26-28)

The production of PSS is typically carried out *via* sulfonation of polystyrene using concentrated sulfuric acid,(29, 30) acetyl sulfate(8) or gaseous sulfur trioxide.(31) Alternatively, controlled radical polymerisation processes, such as Atom Transfer Radical Polymerization (ATRP),(32, 33) Nitroxide-Mediated Polymerisation (NMP),(34-36) and Reversible Addition–Fragmentation chain Transfer (RAFT) polymerisation,(36-39) have been revolutionary for the production of well-defined macromolecules with predetermined molecular weight. Accordingly, these techniques have been exploited to obtain PSS with low molar mass dispersity when directly polymerised from the corresponding sodium *p*-styrene sulfonate monomer *via* NMP,(11, 40, 41) ATRP,(42-44) and RAFT.(37, 45, 46)

However, synthesis of PSS containing copolymers by post sulfonation of polystyrene using sulfonating agents is not easily controllable, especially at high sulfonation levels, due to the extremely different polarity between block segments.(47) Similarly, the incorporation of poly (*p*-styrene sulfonate) into hybrid materials with disparate polarities, such as

amphiphilic block copolymers,(48-50) can be challenging due to the differing nature of constituents and the difficulty in finding a common solvent system. To circumvent this problem, Okamura *et al.*(51) reported a novel approach to produce amphiphilic PSS-containing copolymers by synthesising a sulfonate ester precursor, neopentyl *p*-styrene sulfonate (NSS) and converting it into its sulfonic derivative, either chemically or by thermal treatment, post polymerisation. This strategy was subsequently adopted by several groups to produce PSS-containing copolymers using different types of controlled radical polymerisation techniques; NMP,(52-54) ATRP,(47, 55-57) and RAFT(50) for a wide range of applications. Given that this approach allows the use of common organic solvents during polymer synthesis, the material can be easily combined with other hydrophobic components, subsequently processed into thin films, and finally deprotected to restore the hydrophilic, ionic character of the sulfonic acid group. This procedure is therefore of great relevance to avoid the aforementioned processing problems reported for organic electronics.(28)

Among the different researchers implementing this strategy, Thelakkat's group demonstrated the RAFT polymerisation of NSS for the first time to produce novel block copolymers for use in organic photovoltaics.(50) Motivated by this work, and the clear importance of this thermally-processable polymer in OPV and other aforementioned fields, we extended the study to identify the most effective RAFT polymerisation route of NSS. In the present work, we describe the controlled RAFT polymerisation of NSS under a range of conditions to identify an optimum system for producing well-defined PNSS with a systematically variable degree of polymerisation over a controlled molecular weight range

(Figure 1a). To this end, two different CTAs, namely 2-azidoethyl 3-benzylsulfanylthiocarbonylsulfanylpropionate (BTTC-N₃) and 2-azidoethyl 2-(dodecylthiocarbonothioylthio)-2-methylpropionate (DTTC-N₃), have been investigated (see Figure 1b), and the effect of temperature (60 *versus* 75 °C), diluent (THF, anisole, toluene) and monomer concentration have also been systematically studied. The most successful polymerisation conditions (4.0 M NSS in anisole at 75 °C using DTTC-N₃ as CTA), were examined further in order to prepare PNSS with varying molecular weights by altering the [NSS]₀:[DTTC-N₃]₀ ratio.

Finally, to demonstrate the utility and versatility of our approach, whilst simultaneously confirming the presence of the azide moiety on the end of our polymer chains, PNSS-N₃ has been clicked to bisalkyne-functionalised polybutadiene, PBD-dialkyne, to produce a hydrophobic block copolymer, PNSS-*b*-PBD-*b*-PNSS. Upon thermolysis, this block copolymer becomes amphiphilic as the PNSS block is deprotected to generate poly(*p*-styrene sulfonate) (PSS) end blocks, as previously shown for PNSS-*b*-poly(*n*-butyl acrylate).⁽⁵⁶⁾ The use of azide-alkyne click chemistry herein opens up this approach to a whole host of hydrophobic polymers, not just those capable of being polymerised by radical chemistries.

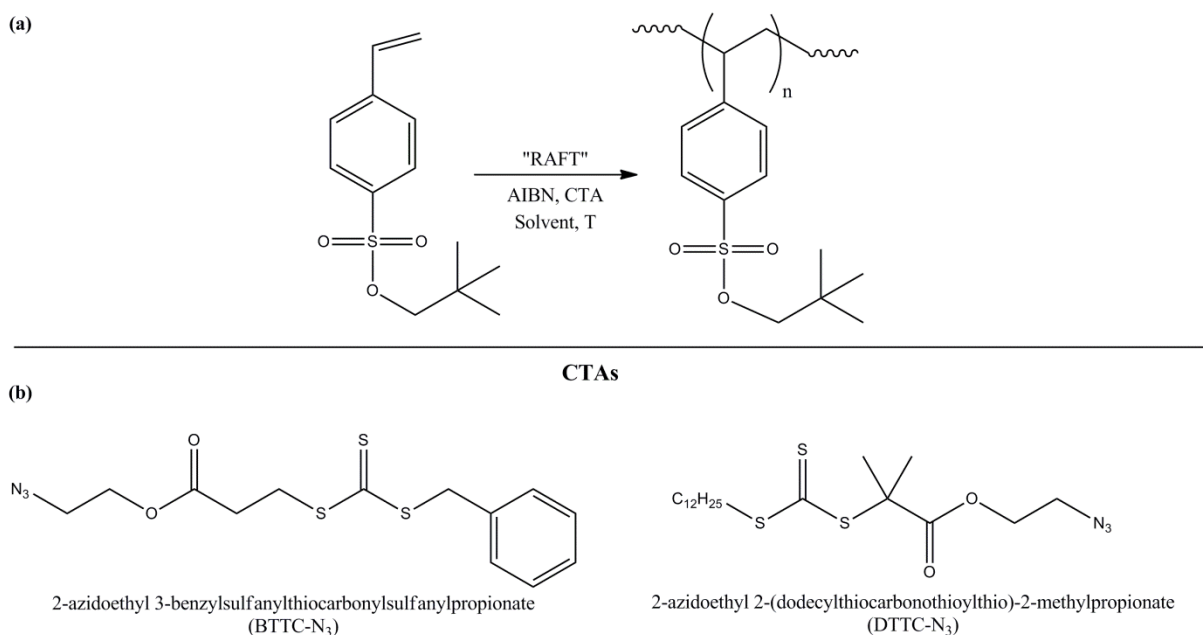


Figure 1. (a) Reaction scheme for the synthesis of poly(neopentyl *p*-styrene sulfonate) and (b) structures of the two chain transfer agents, BTTC-N₃ and DTTC-N₃, trialled in this study.

Experimental Part

Materials

Dimethylformamide (DMF), diethyl ether, methanol (MeOH), dichloromethane (DCM), hexane and ethyl acetate (Laboratory Reagent grade), hexane (Laboratory Reagent grade) were purchased from Fisher Scientific and used as supplied. Sodium chloride (99 %), anhydrous magnesium sulfate (99.5 %), pyridine (99 %) and hydrochloric acid (HCl, 36.5 - 38 %) were purchased from Alfa Aesar, and were all used as received. Thionyl chloride (97 %), sodium-4-styrene sulfonate (technical grade, ≥ 90 %), neopentyl alcohol (99 %), dicarboxy-terminated polybutadiene ($M_n \sim 4,200$; trans-1,4 = 45 – 65 %, cis-1,4 = 20 – 45 %, vinyl = 13 – 30 %), *N,N'*-dicyclohexylcarbodiimide (DCC, 99 %) 4-dimethylaminopyridine (DMAP, ≥ 99 %), propargyl alcohol (99 %), copper(I) iodide (99.999 %), triethylamine (≥ 99.0

%), anhydrous tetrahydrofuran (THF, $\geq 99.9\%$), anhydrous anisole ($\geq 99.9\%$) and anhydrous toluene ($\geq 99.9\%$) were purchased from Sigma Aldrich and used without further purification. Chloroform-d ($99.8\% \text{ At} + 0.05\% \text{ TMS}$, Goss Scientific) and 2,2'-azobis(isobutyronitrile) (AIBN, TCI), were used as supplied. 2-Azidoethanol,(58) 3-benzylsulfanylthiocarbonylsulfanylpropionic acid (BTTC),(59) and 2-azidoethyl 2-(dodecylthiocarbonothioylthio)-2-methylpropionate (DTTC-N₃)(60) were synthesised according to previous literature procedures.

Methods

Monomer synthesis (NSS)

The two-step synthesis of neopentyl *p*-styrene sulfonate (NSS), via *p*-styrene sulfonyl chloride, was performed according to previously reported procedures.(51, 61) The reaction scheme is depicted in Scheme S1 (ESI).

Synthesis of 2-azidoethyl 3-benzylsulfanylthiocarbonylsulfanylpropionate (BTTC-N₃)

3-Benzylsulfanylthiocarbonylsulfanylpropionic acid (BTTC, 15.0 g, 55 mmol), 4-dimethylaminopyridine (3.3 g, 27 mmol) and 2-azidoethanol (9.6 g, 110 mmol) were dissolved in DCM (500 ml). The reaction was stirred for 15 minutes at room temperature under nitrogen, to which a solution of *N,N'*-dicyclohexylcarbodiimide (DCC, 11.3 g, 55 mmol) in DCM (150 ml) was slowly added and the resulting mixture was then stirred at room temperature for 48 h. Following filtration, DCM was removed under reduced pressure and the resulting crude product was purified by column chromatography using hexane:ethyl acetate as eluent (95:5 v/v) to give the azide-functionalised chain transfer agent, BTTC-N₃

(15.6 g, 83 %) as a yellow oil. ^1H NMR in CDCl_3 (δ , ppm): 2.83 (t, 2H, $J = 6.9$ Hz), 3.47 (t, 2H, $J = 5.9$ Hz), 3.65 (t, 2H, $J = 6.9$ Hz), 4.28 (t, 2H, $J = 5.4$ Hz), 4.61 (s, 2H), 7.32 (m, 5H). ^{13}C NMR in CDCl_3 (δ , ppm): 31.1, 33.0, 41.5, 49.7, 63.4, 127.8, 128.8, 129.3, 171.1.

RAFT polymerisation of neopentyl *p*-styrene sulfonate (NSS)

RAFT polymerisation of neopentyl *p*-styrene sulfonate (NSS) was carried out according to the simplified scheme shown in Figure 1a. The great majority of polymerisations undertaken in this work were performed according to initial conditions $[\text{AIBN}]_0/[\text{CTA}]_0/[\text{NSS}]_0 = 0.3/1/20$, indicating a target degree of polymerisation (D_p) of 20. A 25 ml round bottomed flask, equipped with a magnetic follower, was charged with a mixture of NSS (1 g, 4 mmol), AIBN (10 mg, 0.06 mmol), BTTC- N_3 or DTTC- N_3 (0.2 mmol) and anhydrous solvent; THF, anisole or toluene (1, 3 or 5 ml, corresponding to monomer concentrations of 4.0, 1.3 and 0.8 mol dm^{-3} , respectively) under inert atmosphere. The solution was stirred and purged with nitrogen for 15 minutes. Following which, the solution was left under a positive pressure of nitrogen, with stirring, the flask sealed and placed in an oil bath at 60 °C or 75 °C. Aliquots of the solution were taken periodically and the polymerisation was monitored up to high conversion using ^1H NMR spectroscopy and gel permeation chromatography (GPC). Termination proceeded by rapidly cooling the reaction mixture in ice. Subsequently, the reaction mixture was diluted with 2 ml of THF, and the resulting polymer solution was reprecipitated into 150 ml of methanol. The yellowish solid was isolated by filtration and dried under vacuum. ^1H NMR in CDCl_3 (δ , ppm): 0.91 (br, 9H), 1.52 (br, 2H), 1.82 (br, 1H), 3.75 (br, 2H), 6.70 (br, 2H), 7.70 (br, 2H). Selected IR bands (ATR, cm^{-1}): 2951 m, 2947 m,

2883 w, 2116 w, 1743 w, 1595 w, 1482 m, 1418 m, 1352 s, 1310 w, 1281 w, 1179 s, 1097 m, 1072 w, 1050 w, 992 w, 956 s, 947 s, 833 s, 466 m.

Identical procedures were followed for the experiments targeting polymers of D_p 100 and 200, except that the ratio $[AIBN]_0/[CTA]_0/[NSS]_0$ was varied to 0.3/1/100 and 0.3/1/200, respectively.

Synthesis of triblock copolymer, poly(neopentyl *p*-styrene sulfonate)-*block*-polybutadiene-*block*-poly(neopentyl *p*-styrene sulfonate), PNSS-*b*-PBD-*b*-PNSS

The synthesis of bisalkyne-terminated polybutadiene (PBD-dialkyne), is described in the electronic supplementary information (Scheme S2, Figures S8 and S9). To prepare the PNSS-*b*-PBD-*b*-PNSS block copolymer, PBD-dialkyne (200 mg, 47 μmol ; using the M_n value provided by the supplier plus the mass of groups introduced at the termini, 4,278 g mol^{-1} , and not the GPC M_n value of 9,300 g mol^{-1} , which is relative to polystyrene standards), PNSS-N₃ (560 mg, 191 μmol) and CuI (89 mg, 467 μmol) were subjected to three cycles of evacuation and backfilling with N₂ (5 min). THF (20 ml) was added and the mixture was degassed with bubbling N₂ (0.5 h). DIPEA (1.0 ml) was added by syringe and the mixture was stirred at 50 °C for 24 h. The solution was filtered through neutral Al₂O₃ to remove Cu salts, concentrated *in vacuo* to a volume of ca. 5 ml, then poured into MeOH (50 ml) to precipitate the polymer. The polymer was isolated by filtration and dried *in vacuo* (150 mbar, 16 h). Recovery: 190 mg (40.1 %). ¹H NMR (300 MHz, CDCl₃) δ_H , ppm: 0.93 (br s, 18H), 1.10-1.70 (br m, 15H), 2.03 (br s, 46H), 3.24 (br s, 0.14H), 3.75 (br s, 4H), 4.43 (br s, 0.11H), 4.91-4.99 (br m, 5H), 5.22 (br s, H), 5.38-5.56 (br m, 23H), 6.50-7.20 (br m, 4H), 7.50-7.90 (br m, 4H). Selected IR bands (ATR, cm^{-1}): 3087 w, 2920 m, 2846 w, 1740 w, 1646 w, 1601 w, 1481 w,

1451 w, 1420 w, 1360 m, 1314 w, 1279 w, 1180 s, 1103 w, 964 s, 915 m, 832 s, 685 w, 657 m, 587 s, 468 w. GPC (RI): M_n 19,300 g mol⁻¹, M_w/M_n = 1.29.

Thermolysis of poly(neopentyl *p*-styrene sulfonate), PNSS, to poly(*p*-styrene sulfonate), PSS

PNSS-*b*-PBD-*b*-PNSS (25 mg) was dissolved in DCM (750 μl) and a film sample was prepared by depositing 50 μl of the polymer solution onto a glass cover slip. The sample was left in a covered petri dish for 2 h in order to evaporate the majority of the solvent, and residual DCM was removed *in vacuo* (120 mbar, 4 h). Following which, the film was heated at 150 °C for 2 h under a constant flow of N₂ in order to remove the neopentyl protecting groups from the PNSS blocks, generating hydrophilic PSS segments. Selected IR bands for PSS-*b*-PBD-*b*-PSS (ATR, cm⁻¹): 3387 br, 2926 s, 2851 s, 1707 m, 1600 w, 1501 w, 1445 m, 1411 w, 1365 w, 1127 s, 1035 s, 1003 s, 965 s, 909 m, 829 m, 772 w, 674 m, 578 m.

Characterisation

NMR spectroscopy (Bruker Avance ¹H 300 MHz, ¹³C 75 MHz, CDCl₃) was used to determine monomer conversion, whereas polymer molecular weight (M_n) and dispersity (D , M_w/M_n) were measured using gel permeation chromatography (GPC). The GPC systems, operated at 40 °C, and were composed of three PL gel 5 μm 300 x 7.5 mm mixed-C columns or two PL gel 10 μm 300 x 7.5 mm mixed-B columns and one PL gel 5 μm 300 x 7.5 mm mixed-C column. In both cases, degassed THF containing 2 % (v/v) TEA was used as the eluent, at a flow rate of 1 ml min⁻¹. The columns were calibrated with narrow polystyrene standards (M_p = 162 - 6 035 000 g mol⁻¹) and data were analysed using either PL Cirrus software 2.0 or

GPC Analysis software packages, which were both supplied by Agilent Technologies. Fourier transform infrared (FTIR) spectra were accumulated over 16 scans in attenuated total reflectance (ATR) mode using a Thermo Nicolet 380 FTIR spectrophotometer over the range 4000-400 cm^{-1} and a resolution of 4 cm^{-1} . A Mettler Toledo TGA/DSC 1 thermogravimetric analyser (TGA) with StarE software was used to measure the weight changes in PNSS- N_3 and PNSS-*b*-PBD-*b*-PNSS as a function of annealing time at 150 °C. Samples of the materials (ca. 5 mg) were accurately weighed into alumina pans. Isothermal analyses were performed at 150 °C for two hours in a N_2 atmosphere (flow rate: 75 $\text{ml}\cdot\text{min}^{-1}$). The wetting properties of the copolymers were studied using a GBX Digidrop CAM apparatus. Sessile drop static contact angle measurements were made with ultrapure H_2O (Fluka). A drop of pure water (2 μl) was released from the Teflon tip of a syringe onto the sample surface. The equilibrium contact angle (ϑ_e) values reported are the average of 15 measurements taken at three locations on the substrate surface.

Results and Discussion

Several parameters were evaluated in order to optimise the conditions for the preparation of well-defined PNSS using RAFT polymerisation. The effect of chain transfer agent (CTA), monomer concentration, solvent and temperature, on the polymerisation kinetics and the quality of the final polymer, has been assessed systematically, as shown in Table 1.

CTA choice

Initial screening was undertaken to identify a suitable CTA for the RAFT polymerisation of neopentyl *p*-styrene sulfonate (NSS). The CTAs selected were 2-azidoethyl 3-benzylsulfanylthiocarbonylsulfanylpropionate (BTTC- N_3) and 2-azidoethyl 2-

(dodecylthiocarbonothioylthio)-2-methylpropionate (DTTC-N₃), which differed in the Z stabilising group; aliphatic chain (DTTC-N₃) or aliphatic ester with terminal azide functionality (BTTC-N₃) attached to sulfur, and in the R leaving group radical; tertiary (DTTC-N₃) or primary (BTTC-N₃) (as shown in Figure 1b). These trithiocarbonates were selected based on their previous success (in their carboxylic acid or azide-functionalised form) for polymerising more-activated monomers (MAMs), such as styrene,(62, 63) *N,N*-dimethylacrylamide,(62) methyl methacrylate,(63) *N*-isopropylacrylamide,(64-66) ethyl acrylate, acrylic acid, and *N*-*tert*-butyl acrylamide.(67) Furthermore, the azide functionality was designed in our work to furnish each homopolymer with a handle to allow linkage to other materials (*via* click chemistry).(68-71) This provides access to well-defined functional, hybrid or block copolymer materials using facile coupling chemistry of otherwise incompatible building blocks.

<Table 1 near here>

For the initial CTA screening, the RAFT conditions employed were [AIBN]₀/[CTA]₀/[NSS]₀ = 0.3/1/20, at 75 °C, using a monomer concentration of 0.80 M in three different solvents (THF, anisole and toluene). Table 1 (rows 1 to 6) shows the results obtained for the different CTAs. The most noticeable difference is the final polymer molecular weight produced; with BTTC-N₃ affording higher molecular weight PNSS than DTTC-N₃ despite setting identical target degrees of polymerisation. However, regardless of the solvent used, DTTC-N₃ produced polymers with lower dispersities ($\bar{D} \leq 1.14$) and unimodal GPC traces (Figure S1 ESI), whereas BTTC-N₃ afforded PNSS with higher dispersities and, in a number of cases, resulted in GPC peaks with shoulders (Figure S2 ESI). Clearly, the more stable tertiary radical

leaving group, which affords a higher fragmentation rate, offers a higher degree of control over the polymerisation. The final achievable monomer conversion, on the other hand, appears to be independent of CTA in these systems. Both CTAs allow a near identical conversion to be attained when performing the polymerisation in the same solvent.

To extend the screening further, identical experiments were undertaken in THF at a lower temperature (60 °C). Indeed, the same trends were observed (see Figure 2); higher molecular weight polymer was achieved with BTTC-N₃, but with shouldered distributions and higher dispersities throughout the course of the polymerisation. In this case, however, DTTC-N₃ also gave marginally higher monomer conversion (98 % versus 92 %). It is noteworthy that DTTC-N₃ produces a negligible amount of low molecular weight impurities in a number of cases (Figure S1 ESI).

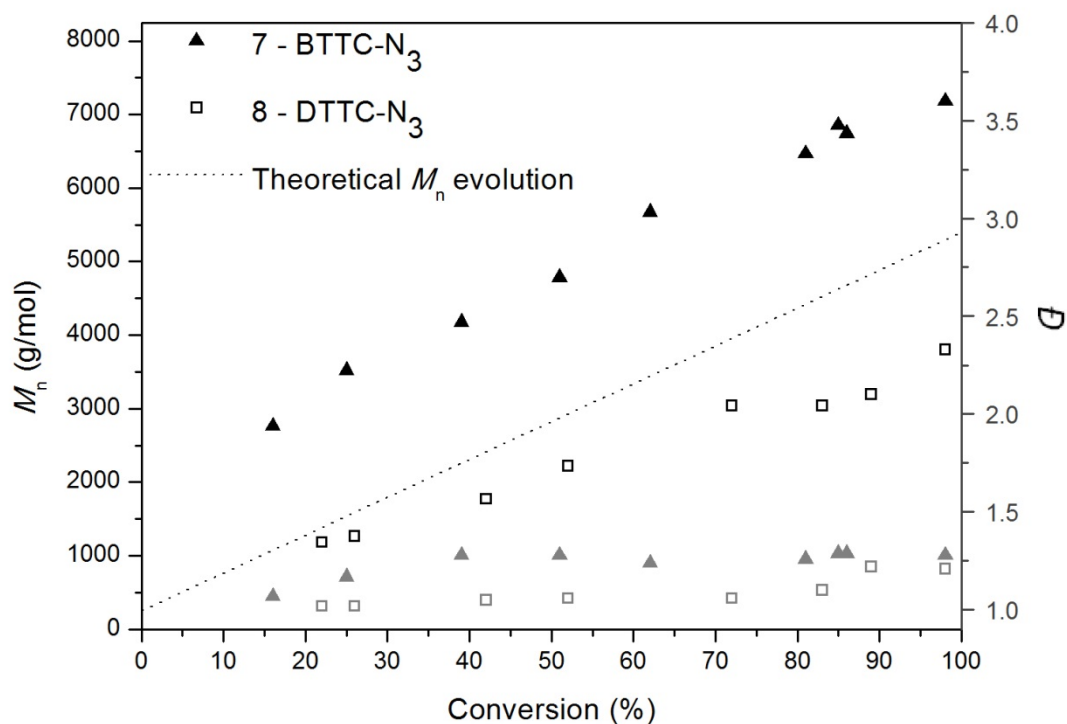


Figure 2. Plot of molecular weight, M_n (black symbols), and dispersity, \mathcal{D} (grey symbols), versus monomer conversion for the polymerisation of neopentyl *p*-styrene sulfonate using BTTC-N₃ (exp. 7) and DTTC-N₃ (exp. 8) in THF at 60 °C. The dotted line indicates the theoretical M_n evolution for the target $D_p = 20$ ($M_n = 5400 \text{ g mol}^{-1}$).

Decreasing the temperature of the reaction led to reduced polymerisation rates compared to the corresponding systems at 75 °C, although better linear fits (for the first order plots) were obtained for both CTAs when the polymerisations were conducted at lower temperatures (Figure 3). In particular, the *pseudo*-first order plot for DTTC-N₃ at 75 °C deviates somewhat from a single linear dependence. At both temperatures, DTTC-N₃ showed higher rates (0.061 h^{-1} at 75 °C and 0.025 h^{-1} at 60 °C) than its primary counterpart BTTC-N₃ (0.041 h^{-1} and 0.021 h^{-1} at 75 °C and 60 °C, respectively). The fits were obtained for the linear regime during the first 48 hours of polymerisation. In summary, DTTC-N₃ was selected for further investigation as it produced PNSS with narrower, and more uniform, molecular weight distributions in all three solvents studied.

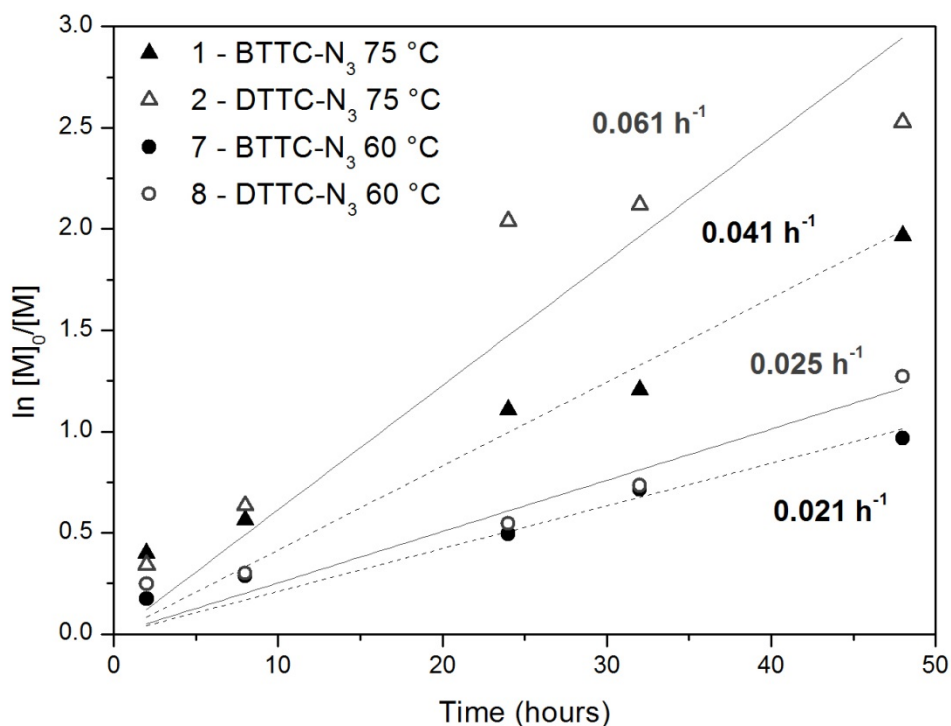


Figure 3. Pseudo-first order kinetic plots for the polymerisation of neopentyl *p*-styrene sulfonate using BTTC-N₃ and DTTC-N₃ in THF at 75 °C (exp. 1 and 2) and 60 °C (exp. 7 and 8), initial monomer concentration 0.80 M.

Monomer concentration

In an attempt to speed up the polymerisation, whilst maintaining control over the final polymer properties, the effect of monomer concentration was studied in the three different solvents (THF, anisole and toluene). In the literature, many articles fail to report the concentration of each species in solution, a parameter which indeed influences the rate of the polymerisation process.⁽⁷²⁾ Interestingly, the scarce reports that do exist on the effect of monomer concentration on the RAFT process show contrasting trends. Wood *et al.*⁽⁷³⁾

compared different amounts of toluene (9.1, 23.1, 41.2, and 66.6 % w/w toluene contents) on the RAFT polymerisation of methyl acrylate. Although they report negligible effects of the dilution in the early stages of polymerisation for the three more concentrated systems, they indicate that the overall rate of polymerisation is significantly lower for the most dilute system, as expected. They also revealed lower monomer conversions for the most dilute system (66.6 % w/w of toluene). Similar results were obtained by Cauët *et al.*(74) for the polymerisation of *p*-acetoxystyrene in 1,4-dioxane. Three concentrations were assessed (33.3, 50 and 66.6 % v/v 1,4-dioxane contents), resulting in lower polymerisation rates for the most diluted systems. They also indicated a slight loss of molecular weight control at higher dilutions. In contrast, Abreu *et al.*(75) report higher monomer conversions at higher dilution for the RAFT polymerisation of vinyl chloride in THF, together with lower molecular weights and higher dispersities. In their study, the solvent contents studied were 50, 75 and 83.3 % (v/v THF contents) and their somewhat anomalous results were attributed to side reactions from the growing macroradicals to the solvent.

In our work herein, the effect of monomer concentration was studied in the three different solvents (THF, anisole and toluene) using DTTC-N₃ at 60 °C. Accordingly, the solvent content was varied from 83.3 % to 75 % and 50 % (w/v solvent content), corresponding to monomer concentrations of 0.80, 1.3 and 4.0 M, respectively (see rows 8 to 16 in Table 1). N.B. these concentrations do not take into account the relatively small quantities of initiator and CTA. Firstly, in THF, high monomer conversions were achieved at all concentrations and the corresponding degrees of polymerisation (ca. 14), approximated by GPC analyses, were close to the target D_p of 20. It should be noted that the molecular weight data obtained

from GPC are relative to PS standards only and, due to differences in the radii of gyration of PNSS and the PS calibrants in THF, absolute molecular weight data are not obtained. Typically, ^1H NMR spectroscopy can be used to determine a more accurate value of M_n for low molecular weight polymers, however this was not possible because CTA peaks were not sufficiently discernable in the polymer NMR spectra. As expected (and in line with the work of Wood *et al.*(73) and Cauët *et al.*(74)) the rate of polymerisation was faster for higher initial monomer concentrations; with less time required to achieve almost complete monomer conversion. Concurrently, the dispersity decreased significantly from 1.21 to 1.07 going from 0.80 to 1.3 M, but then increased slightly to 1.13 in the most concentrated reaction trialled, 4.0 M. Our general trend, however, where diluted systems offer less control over the polymerisation, is more in line with the work of Abreu *et al.*(75) and is attributed to the increased probability of chain transfer to solvent. Although there was no observed change in dispersity of the final polymer, the overall effect of concentration was more pronounced in anisole and toluene than THF, with a marked increase in monomer conversion with increasing monomer concentration, particularly in anisole. Concomitantly, the achieved degrees of polymerisation approached the target D_p as the concentration was increased in all cases. Additionally, the effect of monomer concentration on the apparent rate of polymerisation (k_{app}) was closer to a linear dependence in anisole and toluene (see Figure S3, ESI).

When using the highest concentration (4.0 M), the systems behave similarly, independent of solvent choice, producing polymers close to their target D_p with narrow molecular weight distribution ($\mathcal{D} \sim 1.10$) and high monomer conversions (> 90 %) after only 24 hours in each

case. These more concentrated systems are better suited to industrial applications where the reduced amount of (relatively harmful) solvents and significantly shorter reaction times will reduce costs and the environmental impact of the process.

Solvent effect

In general, the influence of the solvent type used in free radical polymerisation is related to the affinity of the growing polymer radical to the solvent and has a profound effect on the rate of polymerisation. Charge transfer between the macroradical and the solvent has been shown to reduce the rate of addition of incoming monomer and therefore decrease the rate of propagation.(76, 77) On the other hand, reports on the effect of solvent type used in RAFT polymerisation indicate that the influence is insignificant, and often, negligible. For example, Benaglia *et al.*(78) investigated the effect that benzene, acetonitrile, and dimethylformamide had on the RAFT polymerisation of methyl methacrylate mediated by dithiobenzoates. The authors indicate relatively minor effects of the solvent on the process, although slightly lower conversions and \bar{D} were observed in reactions in benzene. Wood *et al.*(73) studied the effect of solvent polarity on the trithiocarbonate-mediated RAFT polymerisation of methyl acrylate, using toluene, *N,N'*-dimethylformamide and methyl ethyl ketone. All systems were shown to exhibit identical *pseudo* first-order rate plots during the early stages of polymerisation. However, for the polymerisation of 2-chloro-1,3-butadiene (CB), our group recently found that the solvent had a marked effect over the control and rate of PCB synthesis, with THF showing an enhanced control over xylene.(79) Similarly, Abreu *et al.*(75) showed distinct differences on the polymerisation of vinyl chloride

performed in dichloromethane, cyclohexanone, and THF; once again with THF giving rise to the most successful results.

According to our data herein, varying results are observed depending on the solvent chosen. The systems with the most polar solvent, THF, were more robust, achieving high monomer conversions and good quality polymers independent of the employed conditions. On the contrary, systems using anisole and toluene were more sensitive to monomer concentration. In these aromatic diluents, higher solvent content suppressed the progress of the polymerisation, particularly at 75 °C, and only permitted 50 - 70 % monomer conversion to be reached. Similarly, at 60 °C, the most dilute anisole system could only attain 70 %, however, the toluene system was actually only marginally affected by dilution, reaching 86 % (instead of 93 % at 4.0 M). In terms of monomer conversion, the general trend of THF > anisole > toluene is observed, which follows the trend of relative polarity. Here, the higher the polarity, the higher the achievable monomer conversions. Concomitantly, the rate of polymerisation (demonstrated by the value of the apparent rate constant for propagation, k_{app}) also follows this dependence. At 60 °C and $[M]_0 = 4.0$ M, reactions using the most polar solvent, THF, had a k_{app} of 0.154 h^{-1} , 0.12 h^{-1} when employing anisole, and 0.064 h^{-1} in the less polar solvent toluene (Figure 4). Although the first order plots are not strictly linear in every case, these trend lines have been selected to display the general rate of the reactions and establish a comparison among the different solvent systems. The reactions in aromatic solvents show similar behaviour during the first 10 hours, and the most significant differences can be observed beyond this timeframe. Our findings are in line with the theory that the higher the affinity of the growing macroradical to the

solvent, the slower the polymerisation. Hence, our relatively non-polar monomer will favour interaction with non-polar solvents giving rise to the observed trends. This theory also helps to explain the lack of sensitivity of the THF system towards changes in initial monomer concentration, compared to the aromatic solvents for which the affinity of the macroradical to solvent is higher.

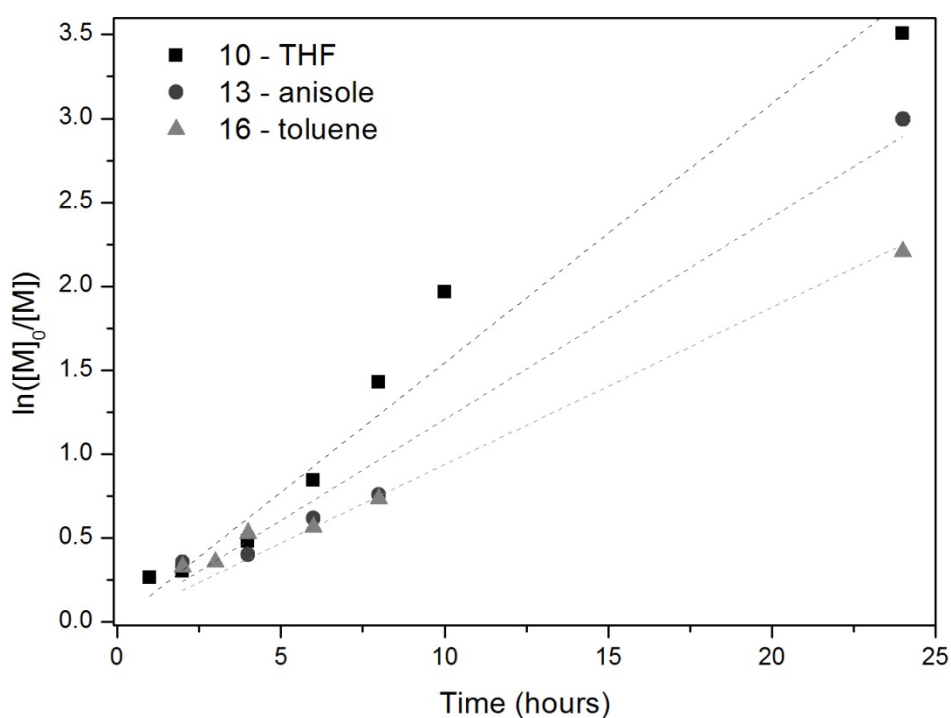


Figure 4. *Pseudo*-first order kinetic plots with DTTC-N₃ at 60 °C, monomer concentration 4.0 M, in THF (exp. 10, ■), anisole (exp. 13, ●) and toluene (exp. 16, ▲).

Overall, the anisole system at the highest concentration (4.0 M) was the most promising in terms of low molar mass dispersity with relatively high monomer conversion. Although this system has been shown to be the most optimum for the polymerisation of neopentyl *p*-

styrene sulfonate, the performance of the other solvents at the same initial monomer concentration was similar and can also be highlighted as acceptable systems for the controlled synthesis of PNSS.

Effect of the temperature

Finally, in a further attempt to reduce polymerisation time, whilst maintaining control over the system, the effect of increasing the temperature to 75 °C was studied in systems at the most effective monomer concentration (4.0 M). It should be noted that only anisole and toluene were investigated under these conditions, as manipulating THF reactions became impractical at such a low dilution and high temperature (THF boiling point = 66 °C). As expected, the results show that the polymerisations are considerably faster at elevated temperature, achieving monomer conversions above 90 % after 8 and 4 hours in anisole and toluene, respectively (compared to 24 hours at 60 °C for both systems). Higher conversions (98 %) could be obtained at longer polymerisation times, however, this came with a loss of control over the system, where distributions became bimodal and dispersities increased significantly (Figures S4 to S6, ESI). Semi-logarithmic plots for these polymerisations (in anisole and toluene at 60 °C and 75 °C) demonstrate linear *pseudo* first-order kinetics, as expected for controlled polymerisation (see Figure 5). In fact, the reactions in anisole and toluene become approximately 4 and 6 times faster, respectively, on moving to 75 °C (Exp. 13, $k = 0.100 \text{ h}^{-1}$; Exp. 17, $k = 0.40 \text{ h}^{-1}$; Exp. 16, $k = 0.100 \text{ h}^{-1}$; Exp. 18, $k = 0.55 \text{ h}^{-1}$). It is clear that increasing the temperature led to enhanced rates and, moreover, improved linear fits in the first eight hours of polymerisation. In summary, increasing the temperature to 75 °C has allowed us to drastically reduce the polymerisation time without compromising control;

high monomer conversion (particularly in anisole) with low molar mass dispersity ($\bar{D} = 1.10$) and moderate agreement of achieved molecular weight with that targeted. Interestingly, for the reactions in toluene at the highest dilution (0.80 M), the decrease in temperature to 60 °C led to better results in terms of both monomer conversion and molecular weight of the obtained polymer (Table 1; rows 6 and 14).

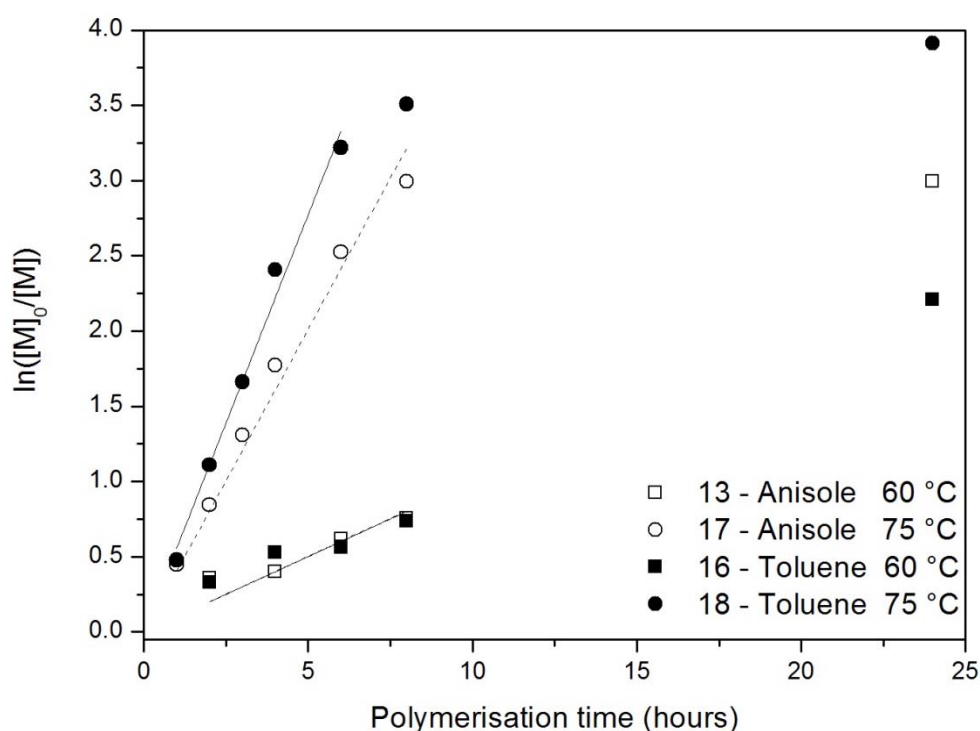


Figure 5. *Pseudo*-first order kinetic plots in anisole (exp. 13, 17) and toluene (exp. 16, 18) at 60 °C and 75 °C. N.B. The trend lines for anisole and toluene are completely coincident within the first 8 hours.

Extending the scope of the polymerisation; effect of $[PNSS]_0:[CTA]_0$ ratio

For the following experiments, the system comprising anisole at 75 °C, with initial monomer concentration of 4.0 M was selected due to its rapidity, linear evolution of the molecular

weight and good quality of the obtained polymer (Figure S7, ESI). This system was employed to synthesise higher molecular weight PNSS with relatively narrow molecular weight distributions. The initial monomer:CTA ratio (target D_p) was modified in order to target polymers of $D_p = 20, 100$ and 200 . Figure 6 shows the GPC traces and molecular weight data of the produced polymers. Indeed, the molar mass dispersity of the polymers increases with molecular weight, yet all afford unimodal distributions over a controlled range of molecular weights. The measured degrees of polymerisation ($D_p = 15, 36$ and 65 , respectively), by GPC, are significantly lower than those targeted, which is partially attributed to differences in the hydrodynamic volumes of PNSS and the PS calibration standards from which these calculations are derived (as aforementioned). Having said this, it is difficult to attribute such vast differences between obtained and theoretical molecular weights to this phenomenon alone and therefore it should be noted that although we can alter the final degree of polymerisation of the polymer by varying the $[\text{monomer}]_0:[\text{CTA}]_0$ ratio, it is difficult to obtain high molecular weight PNSS with the systems reported herein. Nevertheless, the polymerisation conditions identified here produce an extremely versatile material with two key features; a reactive end-group and a thermally responsive protective moiety, that can be exploited for the construction of more complex and structurally diverse materials.

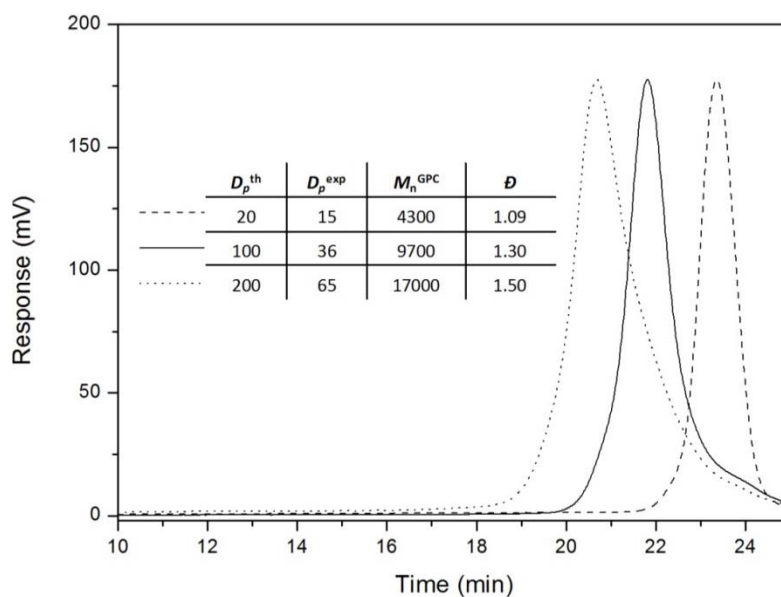
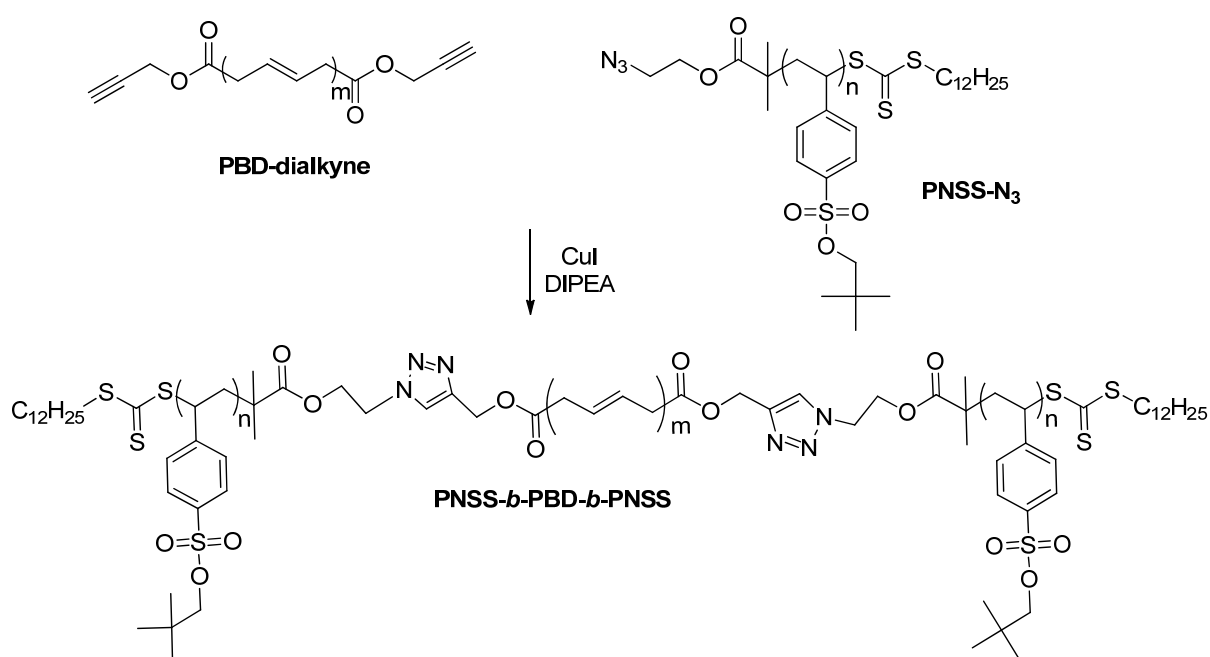


Figure 6. GPC traces of PNSS with varying target molecular weights, synthesised by RAFT using DTTC- N_3 in anisole at 75 °C at 4.0 M NSS. M_n values were calculated relative to polystyrene standards.

Thermolysis of poly(neopentyl *p*-styrene sulfonate), PNSS, to poly(*p*-styrene sulfonate), PSS

In order to briefly demonstrate how the azide-functionalised PNSS (PNSS- N_3) can be utilised for the construction of block copolymers, we prepared a triblock copolymer, poly(neopentyl *p*-styrene sulfonate)-*b*-polybutadiene-*b*-poly(neopentyl *p*-styrene sulfonate) (PNSS-*b*-PBD-*b*-PNSS) (see Scheme 1). The triblock copolymer was then subjected to thermal treatment (150 °C for 2 hours) to convert the PNSS blocks to hydrophilic poly(*p*-styrene sulfonate) segments. For the purposes of clarity and to emphasise the styrene sulfonic acid functionality generated on thermolysis, the thermally treated material is denoted as PSS-*b*-PBD-*b*-PSS. However, it is important to note that the PBD midblock crosslinks during thermal treatment. Copper(I)-catalysed azide-alkyne click chemistry was employed to couple

bisalkyne-functionalised polybutadiene (PBD-dialkyne, $M_n \sim 9,300 \text{ g mol}^{-1}$, $M_w/M_n = 1.76$) to our azide-functionalised PNSS ($M_n \sim 2,600 \text{ g mol}^{-1}$, $M_w/M_n = 1.11$) to yield PNSS-*b*-PBD-*b*-PNSS ($M_n \sim 19,300 \text{ g mol}^{-1}$, $M_w/M_n = 1.29$; it is important to note that although the M_n value of polybutadiene provided by the supplier ($4,278 \text{ g mol}^{-1}$) was used to calculate the reagent stoichiometry for the synthesis of the triblock copolymer, the GPC M_n values here have been used to allow direct comparison between the polymer building blocks and the final copolymer). In the second step, thermolysis of PNSS-*b*-PBD-*b*-PNSS allows one to fabricate amphiphilic copolymer layers from a single organic solvent without the need for post-deposition chemical washes, which is an extremely useful feature for continuous roll-to-roll processing of such polymer films.



Scheme 1. Synthesis of PNSS-*b*-PBD-*b*-PNSS via azide-alkyne click coupling. N.B. Only the major *trans*-1,4 isomer of polybutadiene is shown.

Figure 7 shows the GPC traces and FTIR spectra of the PNSS-N₃ and PBD-dialkyne building blocks along with the resultant triblock copolymer, PNSS-*b*-PBD-*b*-PNSS (¹H NMR spectra are provided in the ESI, Figure S10). Clearly, the GPC traces show the expected unimodal increase in molar mass for the block copolymer, with no detectable homopolymer impurities. Moreover, UV detection (at $\lambda = 270$ nm) confirms that the final triblock copolymer product contains covalently bound, UV-active, PNSS (whereas the GPC traces for PBD alone show no UV-active species). Concomitantly, FTIR characterisation shows that the block copolymer spectrum is a combination of the individual building blocks with the removal of azide and alkyne bands (2116 cm⁻¹ in PNSS-N₃ and 2125 cm⁻¹ in PBD-dialkyne, respectively) as expected. Finally, it should be noted that the efficiency of the click reaction (40.1 %) for this polymer-polymer coupling is moderate, as only a maximum of 77 % of the PNSS chains should be furnished with azide functionality due to the high initiator quantity employed in this work (assuming an initiator efficiency, *f*, of 0.5 for AIBN).

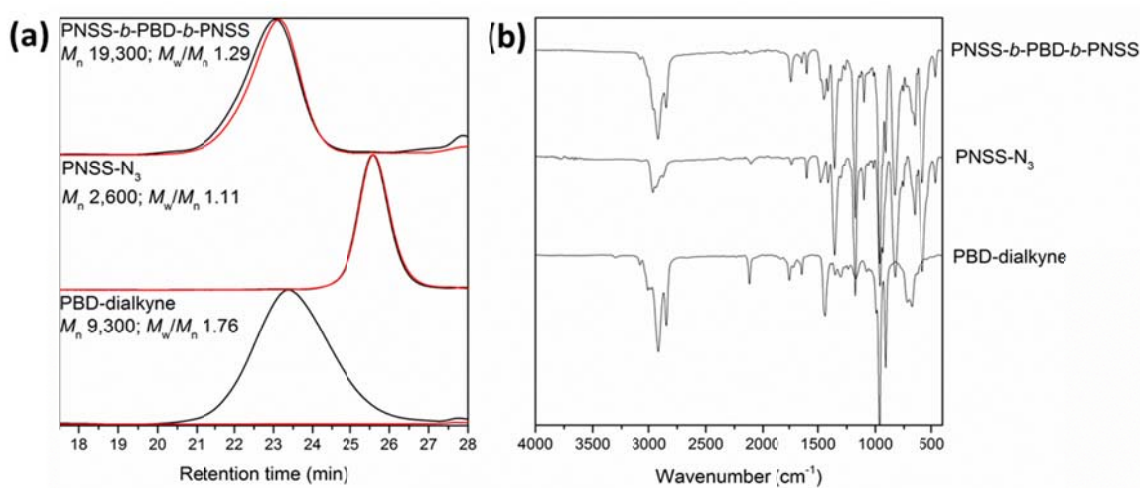


Figure 7. GPC traces (a) and FTIR spectra (b) of the PNSS-*b*-PBD-*b*-PNSS block copolymer and its corresponding building blocks, PNSS-N₃ and PBD-dialkyne. Refractive index signals in the GPC traces (a) are shown in black, while UV signals ($\lambda_{270 \text{ nm}}$) are shown in red.

To confirm the thermal deprotection of the PNSS-*b*-PBD-*b*-PNSS block copolymer to produce an amphiphilic material, thermal gravimetric analysis, TGA, contact angle and FTIR spectroscopy have been employed (see Figure 8). TGA shows a mass loss of 10.9 % for the block copolymer during thermal treatment at 150 °C, which is attributed to the loss of the neopentyl protecting group. The theoretical mass loss for complete removal of the neopentyl group in our block copolymer is 12.6 % and the discrepancy observed herein is attributed to a Friedel-Crafts side reaction, where an extremely small portion of the neopentyl groups are attacked by (and thus attach to) the aromatic rings on the sulfonate repeat units, as reported in the literature.(56, 57) As further proof of the success of the deprotection step, FTIR spectroscopy (Figure 8b) reveals the appearance of a broad band in the region of 3387 cm⁻¹, indicative of the presence of the deprotected sulfonate group, alongside the disappearance of the sulfonate ester group around 1350 cm⁻¹. Following deprotection, the contact angle (with deionised water) decreased slightly from 100.1° ± 0.7° to 95.7° ± 1.6°. While this change represents only a marginal increase in surface hydrophilicity, it is clear from the TGA analysis and infrared spectra in Figure 8 that thermolysis of PNSS-*b*-PBD-*b*-PNSS successfully generates the expected sulfonic acid groups. The small change in the contact angle following thermolysis is therefore attributed to a known phenomenon of molecular reordering of the polybutadiene segments to the hydrophobic air-polymer interface to reduce its free energy.(80)

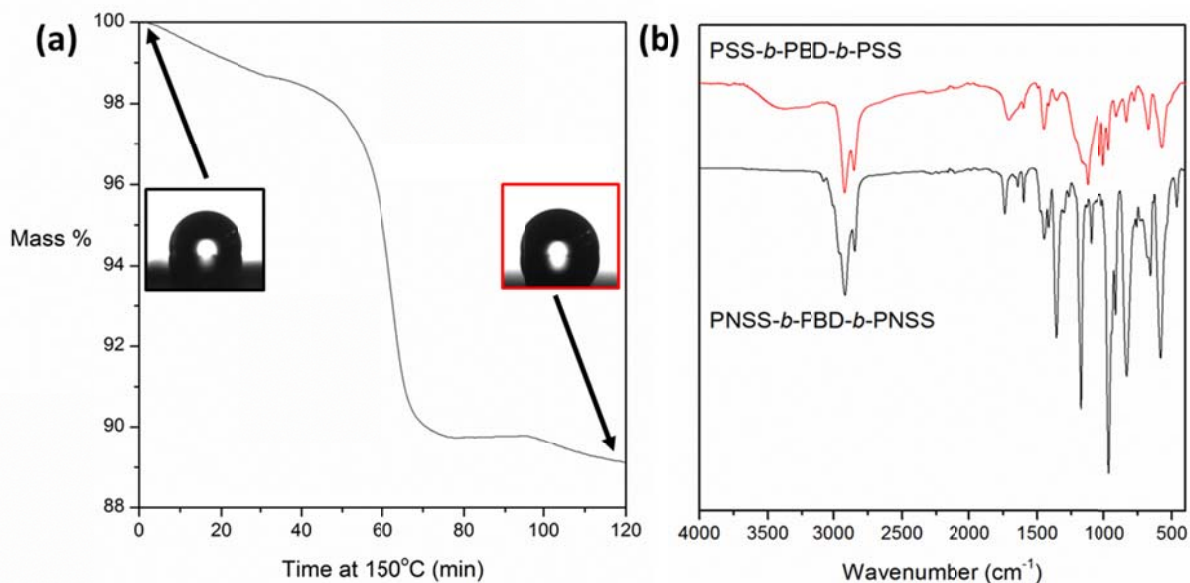


Figure 8. (a) Thermal Gravimetric Analysis during isothermal treatment at 150 °C and contact angle images before (PNSS-*b*-PBD-*b*-PNSS) and after (PSS-*b*-PBD-*b*-PSS) this thermal treatment. (b) FTIR spectra of the PNSS-*b*-PBD-*b*-PNSS and PSS-*b*-PBD-*b*-PSS block copolymers (*i.e.* before and after treatment at 150 °C for 2 hours, respectively). For the purposes of clarity and to emphasise the styrene sulfonic acid functionality generated on thermolysis, the thermally treated material is denoted as PSS-*b*-PBD-*b*-PSS. However, it is important to note that the PBD midblock crosslinks during thermal treatment.

Conclusions

Studies of the RAFT polymerisation of neopentyl *p*-styrene sulfonate have been performed to identify optimum experimental conditions. Two chain transfer agents were trialled, 2-azidoethyl 3-benzylsulfanylthiocarbonylsulfanylpropionate (BTTC-N₃) and 2-azidoethyl 2-(dodecylthiocarbonothioylthio)-2-methylpropionate (DTTC-N₃), where the latter, characterised by a tertiary (and therefore more stable) leaving group with higher fragmentation rates, offered more control as shown by the unimodal GPC traces and lower dispersities of the produced polymers. The effect of the initial monomer concentration (0.8, 1.3 or 4.0 M) was assessed, indicating higher polymerisation rates for more concentrated systems. Faster reactions and higher monomer conversions were observed with the most polar solvent (THF), attributed to the lower affinity of the relatively non-polar monomer radicals for the solvent. Promising results were obtained for the three solvents when [NSS]₀ = 4.0 M, with anisole leading to marginally better dispersity values ($\mathcal{D} < 1.10$). As expected, the polymerisation rate could be increased by increasing the temperature from 60 to 75°C, without compromising control over the process. The most successful conditions ([NSS]₀ = 4.0 M, DTTC-N₃ in anisole at 75 °C) were employed to obtain well-defined PNSS of varied molecular weights with unimodal distributions ($\mathcal{D} \leq 1.50$ in all cases). Finally, to demonstrate the utility of our synthetic approach, a poly(neopentyl *p*-styrene sulfonate)-*b*-polybutadiene-*b*-poly(neopentyl *p*-styrene sulfonate) triblock copolymer was synthesised by azide-alkyne click chemistry (highlighting good retention of the azide functionality on the PNSS chains) and subsequent thermolysis produced an amphiphilic copolymer containing poly(*p*-styrene sulfonate) segments.

Acknowledgements

The research leading to these results has received funding from the European Union Seventh Framework Programme (FP7/2011 under grant agreement ESTABLIS n° 290022).

This work is dedicated to Professor François Schué, who will be sadly missed.

References

1. Ding J, Chuy C, Holdcroft S. *Chemistry of Materials*. **13**: 2231-2233 (2001).
2. Yu J, Yi B, Xing D, Liu F, Shao Z, Fu Y, et al. *Physical Chemistry Chemical Physics*. **5**: 611-615 (2003).
3. Chen S-L, Krishnan L, Srinivasan S, Benziger J, Bocarsly AB. *Journal of Membrane Science*. **243**: 327-333 (2004).
4. Bauman WC, Eichhorn J. *Journal of the American Chemical Society*. **69**: 2830-2836 (1947).
5. Kim J, Kim B, Jung B. *Journal of Membrane Science*. **207**: 129-137 (2002).
6. Athanasekos L, El Sachat A, Pispas S, Riziotis C. *Journal of Polymer Science Part B: Polymer Physics*. **52**: 46-54 (2013).
7. Li D, Jiang Y, Li Y, Yang X, Lu L, Wang X. *Materials Science and Engineering: C*. **11**: 117-119 (2000).
8. Rubinger CPL, Martins CR, De Paoli MA, Rubinger RM. *Sensors and Actuators B: Chemical*. **123**: 42-49 (2007).
9. Al-Marhoun MA, Rahman SS. *Corrosion*. **46**: 778-782 (1990).
10. Saleh MM. *Desalination*. **235**: 319-329 (2009).
11. Bouix M, Gouzi J, Charleux B, Vairon J-P, Guinot P. *Macromolecular Rapid Communications*. **19**: 209-213 (1998).
12. Bélanger DR, Tierney MG, Dickinson G. *Annals of Emergency Medicine*. **21**: 1312-1315 (1992).
13. Antipina MN, Sukhorukov GB. *Advanced Drug Delivery Reviews*. **63**: 716-729 (2011).
14. Watson MA, Baker TP, Nguyen A, Sebastianelli ME, Stewart HL, Oliver DK, et al. *American Journal of Kidney Diseases*. **60**: 409-416 (2012).
15. Girard J, Brunetto PS, Braissant O, Rajacic Z, Khanna N, Landmann R, et al. *Comptes Rendus Chimie*. **16**: 550-556 (2013).
16. Qu L, Shi G. *Journal of Polymer Science Part A: Polymer Chemistry*. **42**: 3170-3177 (2004).
17. Guimard NK, Gomez N, Schmidt CE. *Progress in Polymer Science*. **32**: 876-921 (2007).
18. Andreoli E, Liao K-S, Haldar A, Alley NJ, Curran SA. *Synthetic Metals*. **185-186**: 71-78 (2013).
19. Wei J, Xiong S, Bai Y, Jia P, Ma J, Lu X. *Solar Energy Materials and Solar Cells*. **99**: 141-147 (2012).
20. Kirchmeyer S, Reuter K. *Journal of Materials Chemistry*. **15**: 2077-2088 (2005).
21. Zhang M, Lin P, Yang M, Yan F. *Biochimica et Biophysica Acta (BBA) - General Subjects*. **1830**: 4402-4406 (2013).
22. Hu Z, Zhang J, Hao Z, Zhao Y. *Solar Energy Materials and Solar Cells*. **95**: 2763-2767 (2011).
23. Nguyen TP, Le Rendu P, Long PD, De Vos SA. *Surface and Coatings Technology*. **180-181**: 646-649 (2004).
24. Ghosh S, Inganäs O. *Synthetic Metals*. **101**: 413-416 (1999).

25. Fehse K, Walzer K, Leo K, Lövenich W, Elschner A. *Advanced Materials*. **19**: 441-444 (2007).
26. Dennler G, Scharber MC, Brabec CJ. *Advanced Materials*. **21**: 1323-1338 (2009).
27. Guo X, Baumgarten M, Müllen K. *Progress in Polymer Science*. **38**: 1832-1908 (2013).
28. Jørgensen M, Norrman K, Gevorgyan SA, Tromholt T, Andreasen B, Krebs FC. *Advanced Materials*. **24**: 580-612 (2012).
29. Gibson HW, Bailey FC. *Macromolecules*. **13**: 34-41 (1980).
30. Akovali G, Ozkan A. *Polymer*. **27**: 1277-1280 (1986).
31. Kucera F, Jancar J. *Polymer Engineering & Science*. **49**: 1839-1845 (2009).
32. Wang J-S, Matyjaszewski K. *Macromolecules*. **28**: 7901-7910 (1995).
33. Ando T, Kato M, Kamigaito M, Sawamoto M. *Macromolecules*. **29**: 1070-1072 (1996).
34. Georges MK, Veregin RPN, Kazmaier PM, Hamer GK. *Macromolecules*. **26**: 2987-2988 (1993).
35. Solomon DH. *Journal of Polymer Science Part A: Polymer Chemistry*. **43**: 5748-5764 (2005).
36. Moad G, Rizzardo E, Thang SH. *Accounts of Chemical Research*. **41**: 1133-1142 (2008).
37. Chiefari J, Chong YK, Ercole F, Krstina J, Jeffery J, Le TPT, et al. *Macromolecules*. **31**: 5559-5562 (1998).
38. Moad G, Rizzardo E, Thang SH. *Australian Journal of Chemistry*. **62**: 1402-1472 (2009).
39. Moad G, Rizzardo E, Thang SH. *Australian Journal of Chemistry*. **58**: 379-410 (2005).
40. Keoshkerian B, Georges MK, Boilsboissier D. *Macromolecules*. **28**: 6381-6382 (1995).
41. Mannan A, Fukuda K, Miura Y. *Polymer Journal*. **39**: 500-501 (2007).
42. Wang XS, Jackson RA, Armes SP. *Macromolecules*. **33**: 255-257 (1999).
43. Choi C-K, Kim Y-B. *Polymer Bulletin*. **49**: 433-439 (2003).
44. Iddon PD, Robinson KL, Armes SP. *Polymer*. **45**: 759-768 (2004).
45. Mitsukami Y, Donovan MS, Lowe AB, McCormick CL. *Macromolecules*. **34**: 2248-2256 (2001).
46. Sumerlin BS, Lowe AB, Stroud PA, Zhang P, Urban MW, McCormick CL. *Langmuir*. **19**: 5559-5562 (2003).
47. Baek K-Y. *Journal of Polymer Science Part A: Polymer Chemistry*. **46**: 5991-5998 (2008).
48. Kollisch HS, Barner-Kowollik C, Ritter H. *Chemical Communications*. 1097-1099 (2009).
49. Brusseau S, D'Agosto F, Magnet S, Couvreur L, Chamignon C, Charleux B. *Macromolecules*. **44**: 5590-5598 (2011).
50. Brendel JC, Burchardt H, Thelakkat M. *Journal of Materials Chemistry*. **22**: 24386-24393 (2012).
51. Okamura H, Takatori Y, Tsunooka M, Shirai M. *Polymer*. **43**: 3155-3162 (2002).
52. Matsumoto K, Hasegawa H, Matsuoka H. *Tetrahedron*. **60**: 7197-7204 (2004).
53. Matsumoto K, Hirabayashi T, Harada T, Matsuoka H. *Macromolecules*. **38**: 9957-9962 (2005).
54. Matsumoto K, Kage S, Matsuoka H. *Journal of Polymer Science Part A: Polymer Chemistry*. **45**: 1316-1323 (2007).
55. Baek K-Y. *Molecular Crystals and Liquid Crystals*. **520**: 256/[532]-261/[537] (2010).
56. Baek K-Y, Kim H-J, Lee S-H, Cho K-Y, Kim HT, Hwang SS. *Macromolecular Chemistry and Physics*. **211**: 613-617 (2010).
57. Li X, Jiang Y, Shuai L, Wang L, Meng L, Mu X. *Journal of Materials Chemistry*. **22**: 1283-1289 (2012).
58. Zhu J, Zhu X, Kang ET, Neoh KG. *Polymer*. **48**: 6992-6999 (2007).
59. Stenzel MH, Davis TP. *Journal of Polymer Science Part A: Polymer Chemistry*. **40**: 4498-4512 (2002).
60. Vora A, Singh K, Webster DC. *Polymer*. **50**: 2768-2774 (2009).
61. Schuh K, Prucker O, Rühle J. *Macromolecules*. **41**: 9284-9289 (2008).
62. Gondi SR, Vogt AP, Sumerlin BS. *Macromolecules*. **40**: 474-481 (2007).
63. Skey J, O'Reilly RK. *Chemical Communications*. 4183-4185 (2008).

64. Li M, De P, Gondi SR, Sumerlin BS. *Journal of Polymer Science Part a-Polymer Chemistry*. **46**: 5093-5100 (2008).
65. Lowe AB. *Polymer Chemistry*. **1**: 17-36 (2010).
66. Li M, De P, Li H, Sumerlin BS. *Polymer Chemistry*. **1**: 854-859 (2010).
67. Lai JT, Filla D, Shea R. *Macromolecules*. **35**: 6754-6756 (2002).
68. Topham PD, Sandon N, Read ES, Madsen J, Ryan AJ, Armes SP. *Macromolecules*. **41**: 9542-9547 (2008).
69. Binder WH, Sachsenhofer R. *Macromolecular Rapid Communications*. **28**: 15-54 (2007).
70. Vogt AP, Sumerlin BS. *Macromolecules*. **39**: 5286-5292 (2006).
71. Agut W, Taton D, Lecommandoux S. *Macromolecules*. **40**: 5653-5661 (2007).
72. Keddie DJ. *Chemical Society Reviews*. **43**: 496-505 (2014).
73. Wood MR, Duncalf DJ, Findlay P, Rannard SP, Perrier S. *Australian Journal of Chemistry*. **60**: 772-778 (2007).
74. Cauët SI, Wooley KL. *Journal of Polymer Science Part A: Polymer Chemistry*. **48**: 2517-2524 (2010).
75. Abreu CMR, Mendonca PV, Serra AC, Coelho JFJ, Popov AV, Gryn'ova G, et al. *Macromolecules*. **45**: 2200-2208 (2012).
76. Sato T, Shimizu T, Seno M, Tanaka H, Ota T. *Makromolekulare Chemie-Macromolecular Chemistry and Physics*. **193**: 1439-1444 (1992).
77. Sato T, Masaki K, Kondo K, Seno M, Tanaka H. *Polymer Bulletin*. **35**: 345-350 (1995).
78. Benaglia M, Rizzardo E, Alberti A, Guerra M. *Macromolecules*. **38**: 3129-3140 (2005).
79. Pullan N, Liu M, Topham PD. *Polymer Chemistry*. **4**: 2272-2277 (2013).
80. Kimani SM, Hardman SJ, Hutchings LR, Clarke N, Thompson RL. *Soft Matter*. **8**: 3487-3496 (2012).

Table 1. Summary of reaction conditions, molecular weight data, and monomer conversions of the polymerisation of neopentyl *p*-styrene sulfonate.

Exp.	Solvent	Temp °C	[M] mol dm ⁻³	CTA	Time h	M_n^a g mol ⁻¹	$D_p^{a,b}$	\bar{D}^a (M_w/M_n)	Monomer conversion ^c %
1	THF	75	0.80	BTTC-N ₃	96	5600	21	1.26	97
2	THF	75	0.80	DTTC-N ₃	96	4400	17	1.14	98
3	Anisole	75	0.80	BTTC-N ₃	145	4300	16	1.23	67
4	Anisole	75	0.80	DTTC-N ₃	145	2500	8	1.10	60
5	Toluene	75	0.80	BTTC-N ₃	117	4200	15	1.16	52
6	Toluene	75	0.80	DTTC-N ₃	117	2100	7	1.08	53
7	THF	60	0.80	BTTC-N ₃	196	7200	27	1.28	92
8	THF	60	0.80	DTTC-N ₃	196	3800	13	1.21	98
9	THF	60	1.3	DTTC-N ₃	48	4100	14	1.07	99
10	THF	60	4.0	DTTC-N ₃	24	4000	14	1.13	98
11	Anisole	60	0.80	DTTC-N ₃	72	2500	8	1.07	70
12	Anisole	60	1.3	DTTC-N ₃	48	3200	11	1.07	90
13	Anisole	60	4.0	DTTC-N ₃	24	4000	14	1.08	95
14	Toluene	60	0.80	DTTC-N ₃	72	3400	12	1.08	86
15	Toluene	60	1.3	DTTC-N ₃	48	3700	13	1.08	89
16	Toluene	60	4.0	DTTC-N ₃	24	4200	15	1.12	93
17	Anisole	75	4.0	DTTC-N ₃	8	3600	13	1.10	95
18	Toluene	75	4.0	DTTC-N ₃	4	3800	13	1.10	91

(a) Calculated by THF GPC against polystyrene standards;

(b) $D_p = (M_n \text{ polymer} - M_r \text{ CTA})/M_r \text{ monomer}$; and

(c) calculated by ¹H NMR spectroscopy.